01 Feb 2008

High Voltage Charging of a Capacitor Bank

Sergey I. Shkuratov

Jason Baird
Missouri University of Science and Technology, jbaird@mst.edu

Evgueni F. Talantsev

A. V. Ponomarev

et. al. For a complete list of authors, see https://scholarsmine.mst.edu/min_nuceng_facwork/1187

Recommended Citation

S. I. Shkuratov et al., "High Voltage Charging of a Capacitor Bank," *IEEE Transactions on Plasma Science*, Institute of Electrical and Electronics Engineers (IEEE), Feb 2008.
The definitive version is available at https://doi.org/10.1109/TPS.2007.913818

High Voltage Charging of a Capacitor Bank

Sergey I. Shkuratov, *Member, IEEE*, Jason Baird, *Member, IEEE*, Evgueni F. Talantsev, Andrey V. Ponomarev, Larry L. Altgilbers, and Allen H. Stults

***Abstract*—We have demonstrated the feasibility of charging a capacitor bank to a high voltage using an autonomous ultra-compact explosively driven source of prime power. The prime power source is a longitudinally driven shock wave depolarization of a ferroelectric ceramic. The energy-carrying elements of the shock wave ferroelectric generators (FEGs) were poled $Pb(Zr_{52}Ti_{48})O_3$ polycrystalline ceramic disks with 0.35 cm^3 volume. FEGs charged 9 nF, 18 nF, and 36 nF capacitor banks and provided pulsed-power with peak amplitudes up to 0.29 MW. The maximum efficiency of electric charge transfer from shocked $Pb(Zr_{52}Ti_{48})O_3$ elements to a capacitor bank was 46%. We demonstrated experimentally that the FEG-capacitor bank system can perform as an oscillatory circuit. A methodology was developed for numerical simulation of the operation of the FEG-capacitor bank system; the simulation results were in a good agreement with the experimental results.**

***Index Terms*—Charging capacitor bank, explosive pulsed-power, primary power sources, shock depolarization of ferroelectrics.**

I. Introduction

VARIOUS TYPES of pulsed-power generators utilizing capacitive energy storage devices are widely used in pulsed-power technology for various applications including generation of high-power microwaves and charged-particle beams [1]. In these generators, electric energy is provided to the capacitive energy storage from high voltage power sources powered from a conventional 110/220 V-50/60 Hz supply line. The operation theory of these generators and their uses are well developed [1]. Certain modern applications, however, require that the pulsed-power system be autonomous, that is, use no external power supply line. Explosive-driven pulsed-power generators can be considered one of the most compact and high-efficiency autonomous pulsed-power systems [2]. A novel type of autonomous explosive-driven pulsed-power primary source, the shock wave ferromagnetic generator (FMG), was developed recently [3]–[7]. The FMG uses electromagnetic energy stored for infinite periods in high-energy hard ferromagnets. Operation of these devices is based on the fundamental physical effects of longitudinal [3], [4] and transverse [5]–[7] shock wave demagnetization of hard ferri- and ferromagnets. Ultra-compact FMGs (8.5–25 cm^3 in volume) are capable of producing high voltage pulses with amplitudes greater than 20 kV [3]–[6]. We have experimentally demonstrated that miniature FMGs can be used to charge capacitor banks successfully [8]. The FMGs of a 10-cm^3 volume provided pulsed-powers of 35–45 kW over times ranging from 10 to 15 μs.

Ferroelectrics are another class of materials capable of storing electromagnetic energy for an infinite period of time. Studies of physical properties of ferroelectrics under shock wave compression began in the 1960s [9]–[11] and continue at the present time [12]. We recently developed a series of autonomous shock wave ferroelectric generators (FEGs) utilizing the electromagnetic energy stored in ferroelectric materials [13]. The developed FEGs have been successfully combined with a conventional, nonexplosive power-conditioning device [a spiral vector inversion generator (VIG)] [14]. The autonomous FEG-VIG pulsed-power system is capable of generating output voltage pulses with amplitudes exceeding 90 kV and risetimes of 5 ns [14].

As a continuation of these efforts, we have demonstrated a two-stage pulsed-power system based on a shock wave ferroelectric generator as a charging source for a capacitor bank. Comparison is given of the performance of the FEG-capacitor bank system to systems of other types.

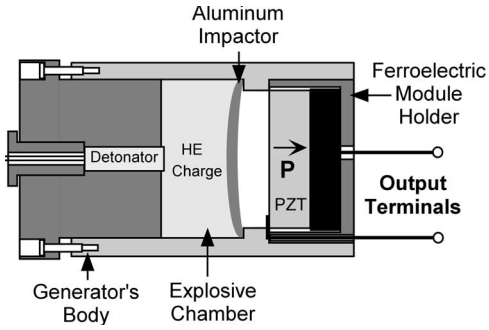

Fig. 1. Schematic diagram of the explosive-driven longitudinal shock wave ferroelectric generator.

II. Experimental Technique

A schematic diagram of the FEG is shown in Fig. 1. The FEG contains a cylindrical body, an explosive chamber, a metallic impactor (flyer plate), and a ferroelectric module. The flyer plate was made of 5052 aluminum (mass 5.1 g). The body and explosive chamber of the generator were made of polycarbonate.

The energy-carrying elements in the FEGs were poled lead zirconate titanate (PZT) $Pb(Zr_{52}Ti_{48})O_3$ polycrystalline piezoelectric ceramic disks (supplied by the EDO Corp. [15]) with

Manuscript received September 3, 2007; revised September 23, 2007.

S. I. Shkuratov, J. Baird, and E. F. Talantsev are with the Loki Inc., Rolla, MO 65409 (e-mail: shkuratov@lokiconsult.com).

A. V. Ponomarev is with the Institute of Electrophysics, Russian Academy of Sciences, Ekaterinburg 620016, Russia.

L. L. Altgilbers and A. H. Stults are with the U.S. Army Space and Missile Command, Huntsville, AL 35807.

Digital Object Identifier 10.1109/TPS.2007.913818

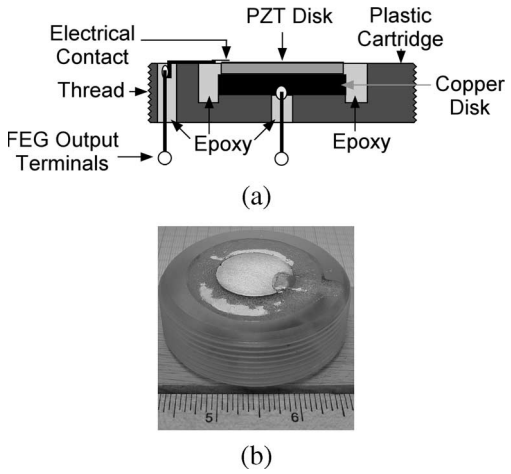

Fig. 2. (a) Schematic diagram of the ferroelectric module holder. (b) Photo of the holder containing $Pb(Zr_{52}Ti_{48})O_3$ energy-carrying elements of $D = 26$ mm and $h = 0.65$ mm.

a diameter of 26 mm and thickness of 0.65 mm (volume 0.35 cm^3). The parameters of the $Pb(Zr_{52}Ti_{48})O_3$ are: density $7.5 \cdot 10^3$ kg/m^3, dielectric constant 1300, Curie temperature 320 °C, Young's modulus $7.8 \cdot 10^{10}$ N/m^2, piezoelectric constant $d_{33} = 295 \cdot 10^{-12}$ C/N, piezoelectric constant $g_{33} = 25 \cdot 10^{-3}$ m^2/C, and remnant polarization $P_0 = 30$ μC/cm^2.

One design problem of high voltage FEGs is the electrical breakdown inside the generator, detailed in [13]. The high voltage breakdown during shock wave depolarization of the ferroelectric material occurs on the side surface of the ferroelectric cylindrical module. A redesign of the ferroelectric module holder (Fig. 2) eliminated the breakdown. The newly designed holder not only prevented the development of high voltage breakdowns but also provided reliable electrical contact between the output terminals and the contact plates of the ferroelectric module. Each generator explosive chamber was loaded with a desensitized RDX high explosive and initiated by a single exploding bridgewire detonator [16].

Explosive experiments were performed at the Explosives Research Laboratory at the University of Missouri-Rolla. Schematic diagrams of the experimental setups are in Fig. 3.

Capacitor banks were made of 1.8 nF ceramic capacitors with nominal voltages of 6.0 kV that were combined into capacitor modules. Each capacitor module combined five ceramic capacitors and was attached to two cylindrical ceramic stands bolted to the bottom of an acrylic measuring box. Each capacitor bank placed in the measuring box contained a certain number of capacitor modules connected in series or parallel.

III. Results and Discussion

Operation of the FEG is as follows. After detonation of the high explosive charge, the aluminum flyer plate is accelerated under the action of a shock wave and high-pressure gases (Fig. 1). The collision of the flyer plate with the ferroelectric disk's front plate initiates a shock wave in the ferroelectric body that propagates through the PZT disk and depolarizes it. The depolarization process releases the induced charge to the metallic contact plates of the ferroelectric disk, and a pulsed

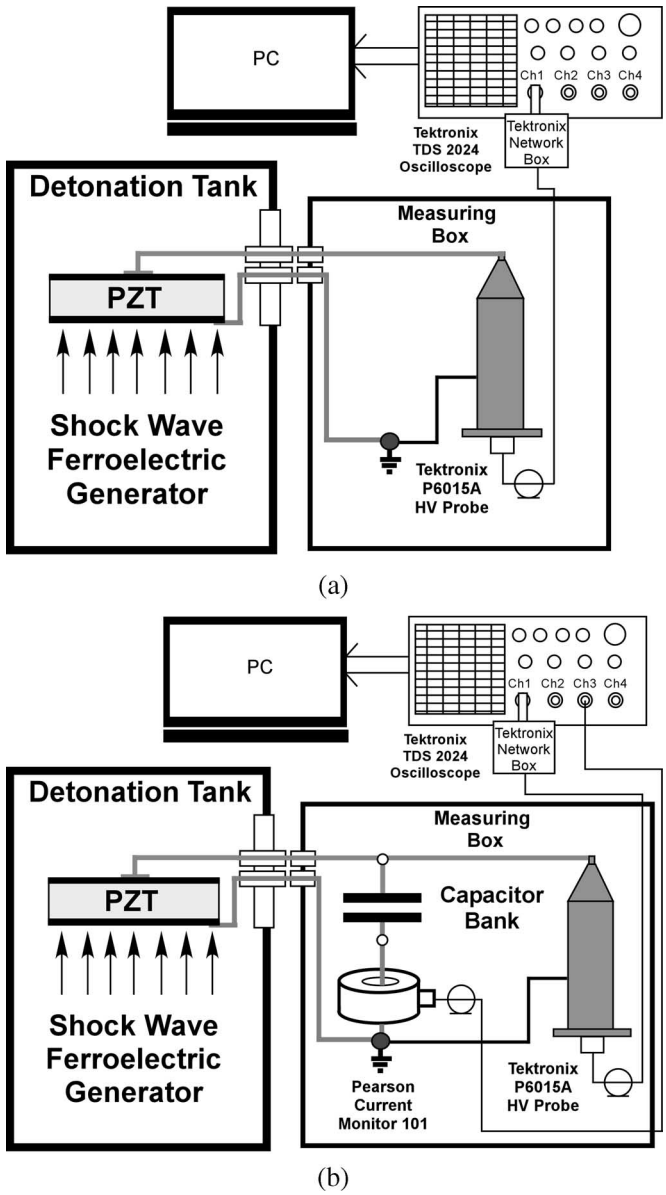

Fig. 3. (a) Schematic diagrams of the measuring system for investigating the operation of FEG in the open circuit mode. (b) FEG–capacitor bank system.

electric potential (electromotive force, EMF) appears on the high voltage output terminals of the generator.

A schematic diagram illustrating the depolarization of a ferroelectric module under longitudinal shock wave impact is shown in Fig. 4. When a longitudinal shock wave (shock wave propagates along the polarization vector $\mathbf{P}_0$) passes through the polarized ferroelectric energy-carrying element, its volume is divided into two parts, or zones, the shock-compressed zone (through which the shock wave has already passed), and the uncompressed zone (through which the shock wave has not passed). The differences between these two zones depend the value of polarization (the compressed zone is depolarized) and other physical properties [9]–[12], [17].

A. Open Circuit Mode

The first series of experiments were performed with FEGs operated in the open circuit mode. A schematic diagram of

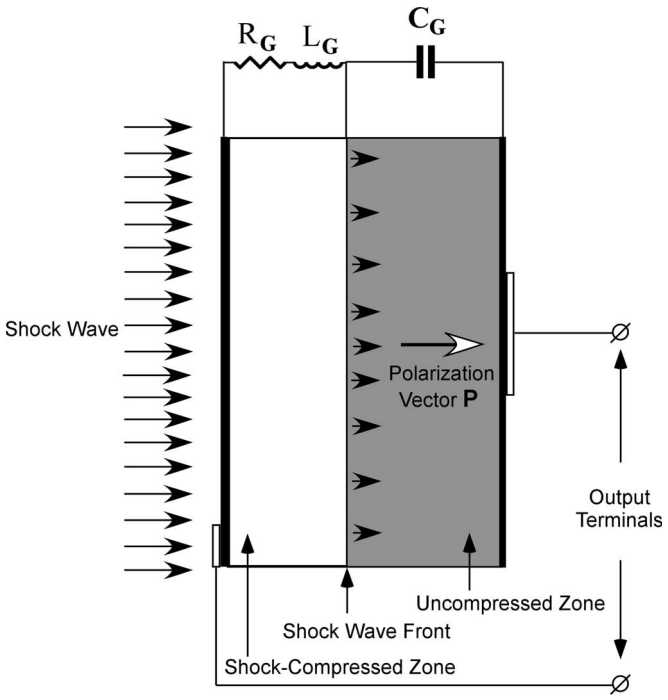

Fig. 4. Schematic diagram illustrating depolarization of PZT module under a longitudinal shock wave impact.

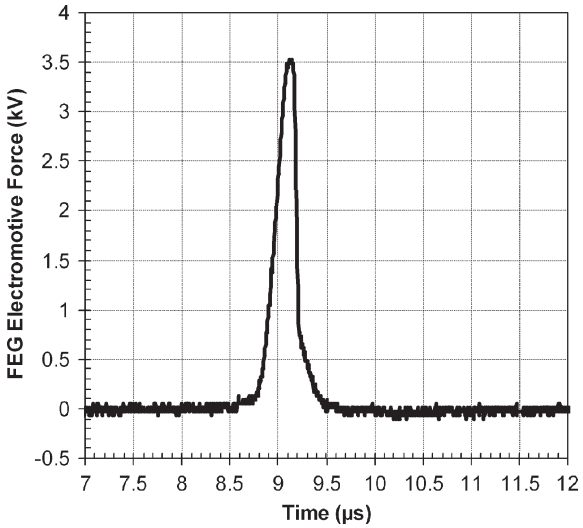

Fig. 5. Waveform of a typical EMF pulse produced by longitudinal shock wave FEG containing a $Pb(Zr_{52}Ti_{48})O_3$ disk of $D = 26$ mm/$h = 0.65$ mm. Open circuit operation.

the experimental setup is shown in Fig. 3(a). The high voltage output terminal of the FEG (positive plate of the PZT energy-carrying element) was connected directly to the input of a Tektronix P6015A high voltage probe. The negative (front) plate of the PZT disk was grounded. We did not use high voltage diodes or high voltage rectifiers in these experiments.

Fig. 5 shows the waveform of the typical pulsed EMF produced by the FEG. The EMF pulse amplitude reached 3.53 kV, the full-width at half maximum (FWHM) was 0.21 μs, and the risetime (τ) from 10% to 90% of the maximum value was 0.25 μs (Fig. 5). The average EMF pulse amplitude in five experiments performed was 3.5 $\pm$ 0.4 kV.

The increase in the EMF pulse from zero to its peak value in Fig. 5 is the direct result of depolarization of the ferroelectric energy-carrying element due to shock wave action. The electrical charge induced due to shock wave depolarization was released to the contact plates of the PZT disk. In this mode of operation, the electric charge was not transferred from the PZT element to the external circuit because of the high resistance and low capacitance of the high voltage probe (100 MΩ/ 3 pF) [Fig. 3(a)]. The charge was utilized for charging the PZT element itself (it is initially a capacitor) to a high voltage. The EMF pulse risetime corresponds to the shock front propagation time through the PZT disk thickness.

After reaching its maximum value the EMF pulse decreases rapidly (see Fig. 5). To understand this phenomenon it is necessary to take into consideration that a shock wave propagating through the ferroelectric energy-carrying element has very complex characteristics [9]–[12], [17]. The wave represents the superposition of a number of elastic and inelastic acoustic and shock waves [12]. These complex waves depolarize the ferroelectric element and change its physical properties significantly [9]–[12], [17]. Apparently, the rapid decrease of the EMF pulse after it reached its peak value (Fig. 5) was the result of a significant increase in the electrical conductivity of the shock-compressed ceramic material (and a corresponding leakage current in the element), or of internal electrical breakdown within the ceramic disk.

B. Capacitor Bank Charging Mode

In the charging mode, the EMF pulse generated by the PZT module due to the shock wave depolarization causes a pulsed electric current, $I(t)$, to flow in the FEG–capacitor bank electrical circuit. In this mode of operation the electric charge induced due to the shock depolarization of PZT was transferred from the PZT element to the capacitor bank.

A schematic diagram of experimental setup for investigations of the FEG–capacitor bank system is shown in Fig. 3(b). The high voltage output of the FEG was connected to the high voltage terminal of the capacitor bank and to the Tektronix P6015A high voltage probe. The negative plate of PZT disk was connected to the ground terminal of the capacitor bank through a Pearson Current Monitor (Model 101). We did not use high voltage diodes or high voltage rectifiers in these experiments.

Integration of the charging current, $I(t)$, waveform from 0 to t gives the momentary value of the electric charge, $\Delta Q(t)$, transferred to the external electrical circuit during explosive operation of the FEG:

$$\Delta Q(t) = \int_0^t I(t)dt. \tag{1}$$

The initial electric charge, Q_0, stored in the PZT energy-carrying elements can be determined as follows:

$$Q_0 = P_0 \cdot A \tag{2}$$

where P_0 is the remnant polarization of the ferroelectric sample and A is its area. Accordingly, PZT disks with $P_0 = 30.4 \pm 1.2$ μC/cm^2 [15] and $A = 5.3$ cm^2 have $Q_0 = 161$ μC.

The first series of FEG–capacitor bank experiments were performed with an 18-nF capacitor bank. This was more than two times higher than the initial capacitance of the FEG, $C_G = 7.0 \pm 0.1$ nF. Fig. 6(a) shows a typical waveform of the high voltage produced by an FEG across an 18-nF capacitor bank. It is not a single pulse but a series of oscillations with a frequency of about 1.0 MHz. The peak voltage amplitude of the first pulse was 2.16 kV, the FWHM of the first pulse was 0.54 μs, and $\tau = 0.34$ μs. The peak energy delivered to the capacitor bank in this experiment [the first pulse in Fig. 6(a)] reached $W(t)_{\max} = C_L U(t)^2_{\max}/2 = 42$ mJ. The average amplitude of the first high voltage pulse produced by the FEG across the capacitor bank in this series of experiments was 2.07 $\pm$ 0.22 kV. The average peak energy delivered to an 18 nF capacitor bank reached 39 $\pm$ 7 mJ.

Fig. 6(b) shows the waveform of $I(t)$ produced by the FEG in the circuit and the circulation of electric charge. The peak amplitude of the first current pulse was 140 A, the FWHM was 0.3 μs and $\tau = 0.52$ μs. The peak amplitude of the second current pulse was higher than the first one and reached 180 A, with FWHM $= 0.45$ μs and $\tau = 0.31$ μs.

It follows from the experiment [Fig. 6(b)] that the electric charge transferred from a PZT module during explosive operation of the FEG to the capacitor bank, $\Delta Q_{\max} = 50$ μC, is 31.8% of the initial charge stored in the ferroelectric element due to its remnant polarization, $Q_0 = 161$ μC.

Waveforms of the output high voltage, $U(t)$, $I(t)$, and power, $P(t)$, pulses produced by an FEG across an 18-nF capacitor bank are shown in Fig. 6(c). The power dissipated in the load was determined to be $P(t) = I(t) \cdot U(t)$. The peak output power reached 0.24 MW. Note that the peak power produced by the FEG is five to seven times higher than that produced by an ultracompact FMG charging the same capacitor bank [8]. The FMG produces a much longer pulse than the FEG (FWHM $=$ 0.3 μs for the FEG and FWHM $= 8.0$ μs for the FMG).

We did not anticipate the oscillatory behavior of the FEG–capacitor bank system, as the experimental series was merely designed to charge a capacitor bank to a certain level of voltage from an explosive-driven power supply. Originally, we considered the results of the first experiment to be an artifact, so we performed three more experiments with identical FEG–capacitor bank systems. The results of these tests, however, were very similar to those shown in Fig. 6.

The next series of experiments was performed with half as much capacitance, 9 nF, of the capacitor bank. The output voltage oscillated as it did in the experiments with an 18-nF capacitor bank (Fig. 6). The frequency of oscillations was slightly higher, $\sim$1.1–1.2 MHz, in comparison with that obtained with the 18-nF capacitor bank. The average amplitude of the first high voltage pulse produced by the FEG across a 9-nF capacitor bank was 2.41 $\pm$ 0.33 kV. The average peak energy delivered to a 9 nF capacitor bank reached 26 $\pm$ 5 mJ.

It follows from our experiments with 9 nF and 18 nF capacitor banks that increasing the capacitor bank capacitance leads to increased energy transfer from the PZT module to the

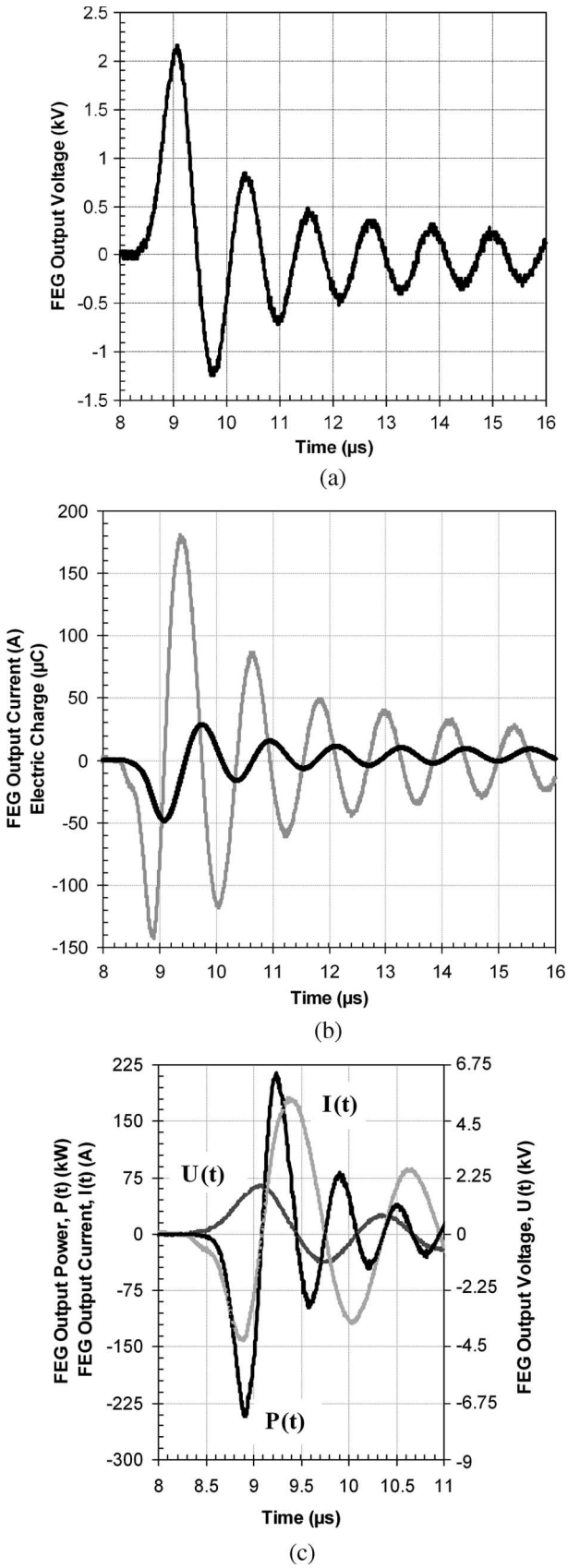

Fig. 6. Typical waveforms of the output voltage, $U(t)$, current, $I(t)$, circulation of electric charge, $\Delta Q(t)$, and power, $P(t)$, produced by the FEG across an 18-nF capacitor bank. (a) Waveform of $U(t)$. (b) Waveform of $I(t)$ (gray), and $\Delta Q(t)$ (black). (c) Waveforms of $U(t)$ (dark gray), $I(t)$ (light gray), and $P(t)$ (black).

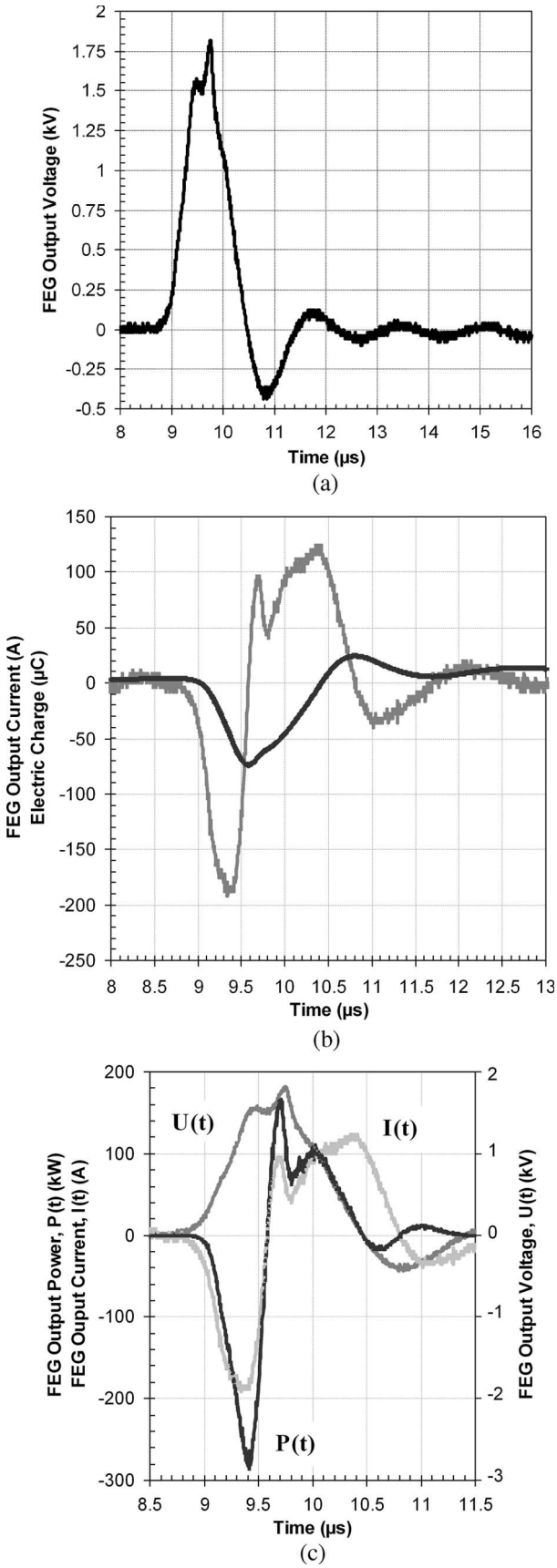

Fig. 7. Typical waveforms of the output voltage, $U(t)$, current, $I(t)$, circulation of electric charge, $\Delta Q(t)$, and power, $P(t)$, produced by the FEG across 36 nF capacitor bank. (a) Waveform of $U(t)$. (b) Waveform of $I(t)$ (gray) and $\Delta Q(t)$ (black). (c) Waveforms of $U(t)$ (dark gray), $I(t)$ (light gray), and $P(t)$ (black).

TABLE I
AMPLITUDE OF MAXIMUM OUTPUT VOLTAGE GENERATED IN AN FEG–CAPACITOR BANK SYSTEM AND ENERGY TRANSFERRED FROM THE FEG MODULE TO THE CAPACITOR BANK AS A FUNCTION OF CAPACITANCE OF THE BANK

Capacitance (nF)	Voltage Amplitude (kV)	Transferred Energy (mJ)
9 nF	2.41 ± 0.33 kV	26 ± 5
18 nF	2.07 ± 0.22 kV	39 ± 7
36 nF	1.75 ± 0.14 kV	55 ± 6

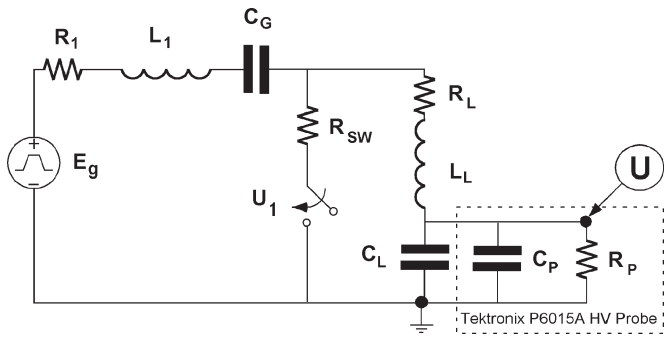

Fig. 8. Equivalent circuit employed for numerical simulation of the FEG–capacitor bank system.

capacitor bank. This result was confirmed in the third series of FEG–capacitor bank experiments, detailed below.

The third series of experiments was performed with a 36 nF capacitor bank. Fig. 7(a) shows a typical waveform of the high voltage produced by an FEG across the bank; note that the results of these experiments were different from those obtained with the 18-nF and 9-nF capacitor banks. The FEG produced a series of oscillations, but the amplitude of the first half-wave is significantly higher than the next one, and the oscillations were damping quickly. The amplitude of the first half-wave of output voltage was 1.82 kV with FWHM $= 0.85$ μs, and $\tau = 0.93$ μs.

The energy delivered to the 36-nF capacitor bank was 60 mJ. From this value we can estimate that the specific energy density of the PZT energy-carrying element was 171 mJ/cm^3. The average amplitude of the first half-wave of high voltage across the 36-nF capacitor bank was 1.75 $\pm$ 0.14 kV, and the average peak energy delivered to the 36-nF capacitor bank reached 55 $\pm$ 6 mJ.

Fig. 7(b) shows the waveform of $I(t)$ produced by the FEG in the circuit, and the circulation of electric charge. The total charge delivered from the PZT energy-carrying element to the 36-nF capacitor bank in this experiment was 73 μC, which is 46% of the initial charge.

Waveforms of the $U(t)$, $I(t)$, and $P(t)$ pulses produced by an FEG across the 36-nF capacitor bank are shown in Fig. 7(c). The peak of output power was 0.29 MW, about eight times higher than that produced by an ultracompact FMG charging the same capacitor bank [8].

It follows from our experimental results that the capacitance of the capacitor bank has a significant effect on the character of processes in the FEG–capacitor bank circuit. The correct choice of capacitor bank capacitance provides maximum output power and maximum energy transfer from the FEG to the external circuit. Table I summarizes the results of our FEG–capacitor bank experiments for all three capacitance levels.

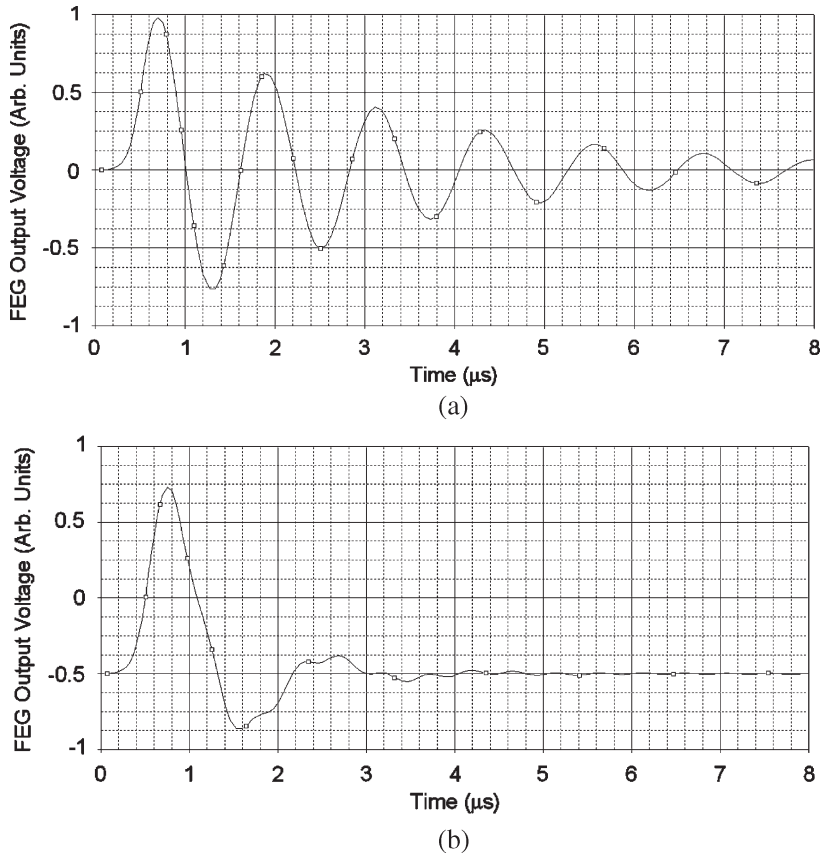

Fig. 9. Results of numerical simulation of operation of an FEG–capacitor bank system. (a) 18 nF capacitor bank. (b) 36 nF capacitor bank.

As mentioned above, we did not expect the oscillatory behavior of the FEG–capacitor bank systems, and at the time we did not understand the cause of these oscillations. In order to understand the physical nature of the oscillations we developed a computer model of the FEG–capacitor bank system that helped us to describe the basic physical mechanism of the observed oscillations.

C. Model of an FEG–Capacitor Bank System

We developed a model of the FEG–capacitor bank system for numerical simulations. The equivalent circuit employed in the simulation is shown in Fig. 8. The shock-compressed part of the ferroelectric energy-carrying element is represented in the equivalent circuit as inductance, L_1, and resistance, R_1.The uncompressed part is represented as C_G. L_1 and R_1 are connected in series to C_G.The inductance, resistance, and capacitance of the load (capacitor bank) and connecting cables are represented in the equivalent circuit as L_L, R_L, and C_L, respectively. The capacitance and resistance of the Tektronix P6015A high voltage probe are represented in the circuit as $C_P = 3$ pF and $R_P = 100$ MΩ, respectively. The internal electrical breakdown in the PZT element is simulated with switch U_1 having resistance R_{sw}. It closes when the voltage across the capacitor bank reaches its maximum value.

The results of the simulation for the 18-nF capacitor bank are shown in Fig. 9(a). The voltage across the bank oscillates as it did in the experiment (Fig. 6). The parameters of the system were as follows: $C_G = 7$ nF, $L_1 = 5$ μH, $R_1 = 0.2$ Ω, $C_L = 18$ nF, $L_L = 2$ μH, $R_L = 2$ Ω, $R_{sw} = 0.3$ Ω.

The results of the simulation for the 36-nF capacitor bank are shown in Fig. 9(b). The parameters of the system, C_G, L_1, R_1, L_L, and R_L, were equal to those for the case with the 18-nF capacitor bank, but C_L was 36 nF and R_{sw} was 4.3 Ω. The output voltage of the FEG was 20% lower than in case of an 18-nF bank [Fig. 9(b)], and it was practically a single pulse as it was in the experiment (Fig. 7).

Based on the results of numerical simulations, we conclude that a key parameter responsible for the oscillatory mode of operation of FEG–capacitor bank system is the resistance of the PZT element after shock compression and internal electrical breakdown. This means that the intensity of the internal electrical breakdown in the shock-compressed PZT module has a significant effect on the processes in the FEG–capacitor bank system.

In the experiments described above, increasing the capacitance of the capacitor bank led to a decrease in the voltage produced by the FEG across the bank and, correspondingly, a decrease in the voltage applied to the shock-compressed ceramic disk. Increased capacitance also had a significant effect on the intensity of electrical breakdown in the PZT. Decreasing the voltage across the capacitor bank below a threshold level results in higher impedances of the conductive channels formed in the ceramics due to electrical breakdown, and it correspondingly causes the aperiodic behavior of signals in the FEG–capacitor bank system.

IV. Summary

We demonstrated that it is fundamentally possible to pulse charge a capacitor bank with a miniature explosive-driven high voltage generator based on the longitudinal shock wave depolarization of poled $Pb(Zr_{52}Ti_{48})O_3$ piezoelectric ceramics.

We showed experimentally that a charge transfer from the longitudinal-shock-compressed PZT energy-carrying element to the capacitor bank can reach 46%. The peak power produced by the longitudinal shock wave ferroelectric generator in the load (capacitor bank) was 0.29 MW. The specific energy density of the PZT module transferred to the capacitor load was 171 mJ/cm^3.

We developed methodology for numerical simulation of the operation of the FEG, and the simulation results were in good agreement with our experimental results.

We demonstrated both experimentally and in simulations that the FEG–capacitor bank system can perform as an oscillatory circuit. The nature of these oscillations appears related to the physics of self-electrical breakdown of shock-compressed poled PZT piezoelectric ceramics.

References

[1] G. A. Mesyats, *Pulsed Power*. New York: Plenum, 2005.

[2] L. L. Altgilbers, M. D. J. Brown, I. Grishnaev, B. M. Novac, I. R. Smith, I. Tkach, and Y. Tkach, *Magnetocumulative Generators*. New York: Springer-Verlag, 2000.

[3] S. I. Shkuratov, E. F. Talantsev, J. C. Dickens, M. Kristiansen, and J. Baird, "Longitudinal-shock-wave compression of $Nd_2Fe_{14}B$ hard ferromagnet: The pressure induced magnetic phase transition," *Appl. Phys. Lett.*, vol. 82, no. 8, pp. 1248–1250, Feb. 2003.

[4] S. I. Shkuratov, E. F. Talantsev, J. C. Dickens, and M. Kristiansen, "Compact explosive-driven generator of primary power based on a longitudinal shock wave demagnetization of hard ferri- and ferromagnets," *IEEE Trans. Plasma Sci.*, vol. 30, no. 5, pp. 1681–1691, Oct. 2002.

[5] S. I. Shkuratov, E. F. Talantsev, J. C. Dickens, and M. Kristiansen, "Transverse shock wave demagnetization of $Nd_2Fe_{14}B$ high-energy hard ferromagnetics," *J. Appl. Phys.*, vol. 92, no. 1, pp. 159–162, Jul. 2002.

[6] S. I. Shkuratov, E. F. Talantsev, J. C. Dickens, and M. Kristiansen, "Ultracompact explosive-driven high-current source of primary power based on shock wave demagnetization of $Nd_2Fe_{14}B$ hard ferromagnetics," *Rev. Sci. Instrum.*, vol. 73, no. 7, pp. 2738–2742, Jul. 2002.

[7] S. I. Shkuratov and E. F. Talantsev, "Powering the coaxial single-turn seed coil of a magnetocumulative generator by an explosive-driven shock wave ferromagnetic primary source," *J. Electromagn. Phenomena*, vol. 3, no. 4, pp. 452–466, Oct.–Dec. 2003.

[8] S. I. Shkuratov, E. F. Talantsev, J. Baird, L. L. Altgilbers, and A. H. Stults, "Compact autonomous explosive-driven pulsed power system based on a capacitive energy storage charged by a high-voltage shock-wave ferromagnetic generator," *Rev. Sci. Instrum.*, vol. 77, no. 6, pp. 066107.1–066107.4, Jun. 2006.

[9] C. E. Reynolds and G. E. Seya, "Two-wave shock structures in the ferroelectric ceramics barium titanate and lead zirconate titanate," *J. Appl. Phys.*, vol. 33, no. 7, pp. 2234–2241, Jul. 1962.

[10] W. J. Halpin, "Current from a shock-loaded short-circuited ferroelectric ceramic disks," *J. Appl. Phys.*, vol. 37, no. 1, pp. 153–163, Jan. 1966.

[11] D. G. Doran, "Shock-wave compression of barium titanate and 95/5 lead zirconate titanate," *J. Appl. Phys.*, vol. 39, no. 1, pp. 40–47, Jan. 1968.

[12] R. E. Setchell, "Shock wave compression of the ferroelectric ceramic $Pb_{0.99}.(Zr_{0.95}Ti_{0.05})_{0.98}Nb_{0.02}O_3$: Hugoniot states and constitutive mechanical properties," *J. Appl. Phys.*, vol. 94, no. 1, pp. 573–588, Jul. 2003.

[13] S. I. Shkuratov, E. F. Talantsev, L. Menon, H. Temkin, J. Baird, and L. L. Altgilbers, "Compact high voltage generator of primary power based on shock wave depolarization of lead zirconate titanate piezoelectric ceramics," *Rev. Sci. Instrum.*, vol. 75, no. 8, pp. 2766–2769, Aug. 2004.

[14] S. I. Shkuratov, E. F. Talantsev, J. Baird, M. F. Rose, Z. Shotts, L. L. Altgilbers, and A. H. Stults, "Completely explosive ultracompact high-voltage nanosecond pulse generating system," *Rev. Sci. Instrum.*, vol. 77, no. 4, pp. 043904-1–043904-5, Apr. 2006.

[15] EDO Electro-Ceramic Products Inc. [Online]. Available: www.edoceramic.com

[16] Reynolds Industries Systems Incorporated. [Online]. Available: www.risi-usa.com

[17] R. F. Trunin, *Shock Compression of Condensed Materials*. Cambridge, U.K.: Cambridge Univ. Press, 1998.

[18] Cadence PCB Design Solutions. [Online]. Available: www.cadencepcb.com, OrCad PCB. [Online]. Available: www.orcadpcb.com, Pspice PCB. [Online]. Available: www.pspicepcb.com

Sergey I. Shkuratov (M'99) was born in 1956 in Achinsk, Russia. He received the M.S. degree in electrical engineering and physics from the Tomsk Institute of Automatic Control Systems and Radioelectronics, Tomsk, Russia, in 1979 and the Ph.D. degree in applied physics from the Institute of High-Current Electronics, USSR Academy of Sciences, Tomsk, Russia in 1987.

In 1986 he joined the Institute of Electrophysics, Russian Academy of Sciences, Ekaterinburg (Sverdlovsk), Russia, as a Research Group Leader. He studied electronic properties, atomic structure, and transport characteristics of high-temperature superconductors; developed high-temperature superconducting switching devices; and conducted materials research for high-efficiency long-life-time electron emission cathodes for high-power microwave devices. From 1998 to 2002, he has been with the Center for Pulsed-Power and Power Electronics at Texas Tech University, Lubbock, where he worked as Associate Research Professor. In 2002 he joined Loki Inc., Rolla, MO, as a Chief Scientist. His current research interests include explosive pulsed-power and high-power microwaves, limitation of electronic components for portable pulsed-power applications, nanoscale research, and engineering.

Dr. Shkuratov is a member of the American Physical Society. He received the USSR Leninsky Komsomol Outstanding Young Scientist Award in 1990 and the Paul Chatterton Award in 1994.

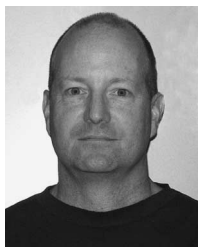

Jason Baird (M'00) was born on 23 December 1955 at Ramey Air Force Base, Puerto Rico. He received the B.S. degree in engineering sciences as an honor graduate at the U.S. Air Force Academy, Colorado Springs, CO, in 1978; the M.S. degree in aeronautical engineering from the U.S. Air Force Institute of Technology at Wright-Patterson Air Force Base, OH, in 1982; and the Ph.D. degree from the University of Missouri-Rolla in 2001.

He retired from the U.S. Air Force as a Lieutenant Colonel in 1991; when he retired, he was the Deputy Director of the Missile Propulsion Division of the Propulsion Directorate, Phillips Laboratory, U.S. Air Force. Since then he has been pursuing studies in energetic materials and shock hydrodynamics at the University of Missouri-Rolla.

Evgueni F. Talantsev was born in 1963 in Kushva, Russia. He received the M.S. degree in physics from the Urals State University, Ekaterinburg, Russia, in 1986 and the Ph.D. degree in physics from the Institute of Physics of Metals, USSR Academy of Sciences, Ekaterinburg (Sverdlovsk), Russia, in 1990.

Since 1986 he was with the Institute of Electrophysics, Russian Academy of Sciences, Ekaterinburg, Russia, where he studied atomic structure, phase transformations, mechanical and emissive properties of metals, ordered alloys, and high-temperature superconductors. From 1998 to 1999, he worked on the E-beam sterilization project at the University of Missouri-Columbia. In 2000, he worked on the scanning atom probe project at the NanoLab at the Kanazawa Institute of Technology, Kanazawa, Japan.

Since 2001 he has been with the Center for Pulsed-Power and Power Electronics at Texas Tech University, Lubbock, where he worked as Assistant Research Professor. In 2003 he joined Loki Inc., Rolla, MO. His current research interests include explosive-driven pulsed-power generators, testing of electronic components for portable pulsed-power applications, and nanoscale research and engineering.

Andrey V. Ponomarev was born in 1962. He received the M.S. degree in electrical engineering from the Tomsk Institute of Automatic Control Systems and Radioelectronics, Tomsk, Russia, in 1984 and the Ph.D. degree in electrical engineering from the Institute of Electrophysics, Russian Academy of Sciences, Ekaterinburg, Russia in 2005.

He has been with the Institute of Electrophysics, Russian Academy of Science, Ekaterinburg, since 1986. His research interests are repetitive pulsed-power, semiconductor opening switches, and high-power solid-state nanosecond pulsed generators.

Larry L. Altgilbers received the Ph.D. in physics from the Semiconductor Physics Institute, Vilnius, Lithuania, where he did research on explosive pulsed-power.

He was employed by the U.S. Army Aviation and Missile Command from 1976 until 1991, where he worked on directed energy weapons and various missile systems. Since 1991, he has been employed by the U.S. Army Space and Missile Defense Command, Redstone Arsenal, AL, where he initially worked on directed energy weapons and is now in the Advanced Technology Directorate. His current duties include managing the development of a variety of technologies through the Small Business Innovative Research Program and the development of pulsed-power and radio frequency technologies.

Dr. Altgilbers is currently a member of the American Physical Society and the American Institute of Aeronautics and Astronautics. He wrote more than 50 conference and journal publications and has published two books: *Magnetocumulative Generators and Unconventional Weapons*.

Allen H. Stults received the B.S. degree in engineering from the U.S. Military Academy, West Point, NY, in 1979. He received the M.S.E. degree from the University of Alabama, Huntsville, in 1998, and the M.B.A. degree from the Florida Institute of Technology, Melbourne, in 1987.

He is currently the Lead Engineer for multifunctional warheads for the Aviation and Missile Research, Development and Engineering Center, Redstone Arsenal, AL.